The Johns Hopkins University
APPLIED PHYSICS LABORATORY
Silver Spring, Maryland

# OUTER ZONE ELECTRONS

by

Donald J. Williams



The Johns Hopkins University

Applied Physics Laboratory

Silver Spring, Maryland

Presented at the Advanced Study Institute, "Radiation Trapped in the Earth's Magnetic Field," August 16 through September 3, 1965, Bergen, Norway.

The Johns Hopkins University
APPLIED PHYSICS LABORATORY
Silver Spring, Maryland

# INTRODUCTION

Satellites in low altitude, high inclination orbits have been used to study near-earth effects of perturbations occurring well out in the magnetosphere by observing the spatial and temporal behavior of energetic electrons. Studies concerned with ≥ 40 kev electrons include: the initial observation of electrons precipitated into the atmosphere from altitudes > 1000 km (O'Brien, 1962); the initial observation of a diurnal variation in the trapped electron population (O'Brien, 1963); further, more detailed studies of trapped and precipitated electrons and their diurnal variations (O'Brien, 1964; O'Brien and Taylor, 1964; McDiarmid and Burrows, 1964 a and b; Frank et al., 1964; Armstrong, 1965); and the recent observation of the existence of "spikes" of 40 kev electrons at latitudes above the boundary of the outer zone and preferentially during local night (McDiarmid and Burrows, 1965). A recent study at 10 kev has shown that intense fluxes of these lower energy electrons occur predominantly at local night and high latitudes (Fritz and Gurnett, 1965).

We present and review in this paper the results of an initial series of studies concerned with the observation and interpretation of the spatial and temporal behavior of high energy ($E_e \geq 280$ kev) trapped electrons in the outer zone. These observations were obtained at low altitude and high latitudes from the polar orbiting satellite 1963 38C.

Differences in the behavior of the lower energy ($\gtrsim 40$ kev) and higher energy ($\gtrsim 280$ kev) electrons have been noted previously (O'Brien, 1964;

Williams and Mead, 1965). It is possible that an improved understanding of the behavior of the low energy electron population may be achieved by a fuller understanding of the high energy electron population. We will present evidence, using the $\gtrsim$ 280 kev electron data obtained from instruments aboard satellite 1963 38C, which leads us to believe that a few characteristic features of the behavior of the high energy electron population in the outer zone can be understood if the distorted geomagnetic field is taken into consideration.

The data concerning $\geq$ 280 kev electrons will be presented in three sections: Dayside variations which show a striking 27 day correlation in trapped electron intensities and appear to be closely related to the passage of the sector boundaries of the interplanetary field as observed by Ness and Wilcox (1965); Diurnal variations which are shown to be consistent with charged particle motion, under conservation of the adiabatic invariants, in a distorted field similar to that measured by IMP-1 (Ness et al., 1964); and Storm-time variations which show that the behavior of these trapped electrons during a main phase magnetic storm is consistent with the simultaneous behavior of the magnetic field in the earth's magnetic tail (Ness and Williams, 1965).

The Johns Hopkins University
APPLIED PHYSICS LABORATORY
Silver Spring, Maryland



## SATELLITE AND DETECTOR

The satellite 1963 38C and the detector of interest have been described in detail previously (Williams and Smith, 1965).

Briefly, the satellite 1963 38C was launched on September 28, 1963 into a nearly circular polar orbit having a 1140 km apogee, a 1067 km perigee, an 89.9° inclination and a 107.5 min. period. Just after launch the satellite orbital plane made an angle of $\sim 6°$ with the noon-midnight meridian and was moving toward the noon-midnight meridian at the approximate rate of 1° per day due to the earth's motion about the sun. The satellite was magnetically aligned and displayed an oscillation of $\lesssim 6°$ about the local line of force some three days after launch.

The experiment of interest is an integral electron spectrometer comprised of five, one millimeter thick, surface barrier solid state detectors. A combination of discriminator levels and absorbing foils yields the spectrometer characteristics shown in Table I. Monitoring an onboard proton spectrometer has shown that proton contamination in these outer zone electron data is negligible.

The spectrometer is oriented to look out normal to the satellite alignment axis. Therefore, after alignment has been achieved the instrument measures the intensity of trapped electrons mirroring at (or very near) the point of observation.

Results from the two lower energy channels, $E_e \geq 280$ kev and $\geq 1.2$ Mev, will be presented in this report. Directional flux levels (#/cm$^2$ sec ster),

The Johns Hopkins University
APPLIED PHYSICS LABORATORY
Silver Spring, Maryland

TABLE I. Electron Spectrometer Characteristics: Oriented 90° to Satellite Alignment Axis

| Detector | Half Angle (deg) | Geometric Factor ($cm^2$ ster) | Foil Thickness ($mg/cm^2$) | Particle Energies yielding pulses between 250 kev and 1 Mev discriminator levels | | |
|---|---|---|---|---|---|---|
| | | | | Electrons | Protons (energies in Mev) | |
| 1 | 6.4 | $2.8(10)^{-3}$ | 10.3 AL | $\geq$ 0.28 Mev | $2.0 \leq E_p \leq 2.3$ | $E_p \geq 178$ Mev |
| 2 | 6.4 | $2.8(10)^{-3}$ | 412 Cu | $\geq$ 1.2 Mev | $14.4 \leq E_p \leq 14.5$ | $E_p \geq 179$ |
| 3 | 6.4 | $2.8(10)^{-3}$ | 946 Cu | $\geq$ 2.4 Mev | $23.27 \leq E_p \leq 23.34$ | $E_p \geq 181$ |
| 4 | 6.4 | $2.8(10)^{-3}$ | 1470 Cu | $\geq$ 3.6 Mev | $30.01 \leq E_p \leq 30.07$ | $E_p \geq 183$ |
| 5 | 3.2 | $4.9(10)^{-4}$ | 10.3 AL | $\geq$ 0.28 Mev | $2.0 \leq E_p \leq 2.3$ | $E_p \geq 178$ |

accurate to $\sim \pm 50\%$, can be obtained by multiplying the $\geq 280$ kev and $\geq 1.2$ Mev count rates by 500 and 1000 respectively.

As of July, 1965 satellite 1963 38C was still in operation and transmitting data of high quality.

## DAYSIDE VARIATIONS

In this section we shall present some data and correlate its behavior with other phenomena. We do not know the mechanisms responsible for the observed particle behavior in this case, even though we can qualitatively predict this behavior given the behavior of an additional parameter, e.g., the $K_p$ values. It appears that to even eliminate certain mechanisms from consideration, simultaneous observations are required, not only of magnetic and particle phenomena, but also at various positions on lines of force throughout the magnetosphere. Hopefully, in the future more use will be made of simultaneous observations to track down the mechanisms responsible for the charged particle behavior throughout the trapping regions.

An initial study of trapped, $\geq$ 280 kev electron intensities, observed on the sunlit hemisphere by satellite 1963 38C, was presented by Williams and Smith (1965). A correlation of trapped electron intensities with magnetic activity (enhanced electron intensities correspond to high $K_p$ values) was presented along with the characteristics of the electron responses to magnetic activity as a function of the magnetic shell parameter, L. Time delays in the electron response to magnetic activity were obtained and found to increase with both increasing energy and L. A rough correlation of the energy spectrum with magnetic activity was obtained, showing that the spectrum becomes softer as the magnetic activity increases.

It was also observed that during times of magnetic quiet, the trapped electron intensities exhibit a steady decay, implying that a steady solar wind does not supply fresh particles to these high latitude ($L \geq 3$), low altitude trapping regions. Perburbations in the trapped particle population seem to occur mainly when the solar wind and/or the interplanetary field direction changes.

It was further observed that electron intensity increases occurred during the time of the 27-day recurring increase in magnetic activity. However, only one solar rotation period was included in the analysis and no definite correlation with a 27-day period could be made.

We have now obtained the trapped, $\geq$ 280 kev electron data at 1100 km on the sunlit hemisphere for the first four solar rotation periods after the launch of 1963 38C. The solar rotations analyzed are the four beginning on October 6, 1963, November 2, 1963, November 29, 1963, and December 26, 1963. The data show a definite 27-day periodicity in that the high energy ($E_e \geq 280$ kev) trapped electrons throughout much of the outer zone ($L \geq 3.5$ at 1100 km) undergo an intensity increase every 27 days coincident with the recurring magnetic activity.

This is shown in Figures 1 and 2 where the trapped electron intensities at $L = 4.5$ are displayed for $E_e \geq 280$ kev and $E_e \geq 1.2$ Mev respectively, for the four consecutive solar rotations beginning October 6, 1963. The data have been reduced as intensity (counts per sec) versus time plots at half integral values of L from $L = 3.0$ to $L = 8.0$. The $L = 4.5$ shell is shown as being typical of the center of the outer zone. Shown along with

the electron data are the 3 hour averages of $K_p$. The correspondence between the electron intensities and magnetic activity is readily discernible.

During the latter two solar rotation periods shown in Figures 1 and 2, November 29 and December 26, 1963, the magnetometers aboard the NASA IMP-1 satellite were able to monitor the interplanetary magnetic field. For these two solar rotations plus the succeeding rotation beginning January 22, 1963, Ness and Wilcox (1965) have reported the existence of a regular longitudinal sector structure in the interplanetary field. The total longitudinal structure co-rotates with the sun and is separated into four sectors. In two of these sectors, each occupying about 2/7 of the total longitude, the field is directed away (+) from the sun. In the two remaining sectors, 2/7 and 1/7 of the total longitude, the field is directed toward (-) the sun. The sector boundaries are neutral sheets separating regions of oppositely directed field and produce, as they sweep past the earth, a rapidly changing transistional field configuration which may interact with the magnetosphere and its environs.

The sector boundaries as measured by Ness and Wilcox (1965), are included in the plots of Figures 1 and 2, and it can be seen that the increase in trapped electron intensities observed near the beginning of a solar rotation, occur at or just after the arrival of a sector boundary. It is interesting to note that for the rotations of November 2, November 29, and December 26, 1963, there is an additional particle increase at the arrival of the sector boundary located $\sim 180^\circ$ from the initial particle increases. The passage of both of these boundaries produces a similar transistional field, i.e., the field changes from - to +. The latter portion of the

October 6 rotation was obscured by two large storms and thus does not exhibit this effect.

These results show clearly the fact that the trapping region is very sensitive to conditions in the interplanetary medium. Whether the interplanetary field configuration or the solar plasma intensity is the primary trigger for these magnetospheric and particle intensity responses, is not yet known. It is somewhat surprising, though, that these mild perturbations (compared to the storms near solar-maximum) are able to significantly alter the relativistic electron population deep in the magnetosphere ($L = 3.5$).

Finally, we show in Figure 3 a plot of the trapped, $\geq 280$ kev electron intensity at $L = 3.0$ for these solar rotations. No discernable response can be seen at the sector boundaries. Only intense magnetic activity yields particle increases at $L = 3$. This occurs for two storms at the end of October, 1963 and not again until January, 1964. During the relatively quiet periods, the intensities show a steady decay right to the detector count rate threshold.

## DIURNAL VARIATIONS

Measurements of the diurnal shift of trapped, ≥ 280 kev electrons in the outer zone (Williams and Palmer, 1965) showed that these higher energy electrons display a significantly smaller diurnal latitude shift during periods of magnetic quiet than do trapped, ≥ 40 kev electrons in the outer zone. An initial qualitative analysis by Williams and Palmer (1965) suggested that the diurnal shift of the trapped, ≥ 280 kev electrons might be explained by particle motion, under conservation of the adiabatic invariants, in a distorted magnetosphere such as described by Mead (1964).

A recent, more detailed quantitative study of these diurnal shifts (Williams and Mead, 1965) has shown that the addition of a current sheet in the anti-solar hemisphere of Mead's model is found to fit the observed latitude shifts, assuming charged particle motion under the conservation of the adiabatic invariants, $\mu$ and J, and the energy E. The addition of this region of enhanced plasma density in the tail field leads to a quiescent field configuration similar to that recently suggested by Dessler and Juday (1965) and Axford et al. (1965) and recently measured by the magnetometer aboard IMP-1 (Ness, 1965).

We shall briefly review the investigations of Williams and Mead (1965) leading to the result that the behavior, during periods of magnetic quiet, of energetic ($E_e \geq 280$ kev) electrons trapped in the outer zone is consistent with their motion in a distorted magnetosphere similar to that suggested and observed, under the conservation of the adiabatic invariants,

$\mu$ and J, and the energy, E. A recent study of trapped high energy ($E_e \geq 1.6$ Mev) electrons near the geomagnetic equator has lead to a qualitatively similar result (Frank, 1965). In the following section we shall discuss some characteristic features of outer zone electron behavior during magnetically disturbed periods.

Figure 4 shows the noon and midnight latitude profiles, displayed as count rate vs. invariant latitude plots, obtained for the magnetically quiet period October 2 through October 12, 1963. The curves of Figure 4 represent the average values obtained for 47 dayside passes and 28 nightside passes received during this time period (Williams and Palmer, 1965). In this time interval, the satellite orbital plane remained within 8° of noon-midnight meridian.

It can be seen from Figure 4 that both energies, $E_e \geq 280$ kev and $\geq 1.2$ Mev, behave in a similar manner and show a distinct separation of the noon and midnight latitude profiles. To test the hypothesis that this separation is simply a latitude shift of the trapped electron population due to their drift in a distorted magnetosphere under conservation of $\mu$, J and E, the amount of latitude shift was obtained as a function of noon time latitude by obtaining the noon, $\Lambda_D$, and midnight, $\Lambda_N$, latitudes which yield the same trapped electron intensity.

These results are shown in Figure 5 where the amount of shift, $\Delta\Lambda = \Lambda_D - \Lambda_N$, is plotted versus the noontime latitude of observation, $\Lambda_D$. Since the $\geq 1.2$ Mev electron data displayed the same behavior, only the $\geq 280$ kev electron data are shown. Two methods of analyzing the data, for

reasons of accuracy (Williams and Mead, 1965), are shown in Figure 5. The matched pass data are from pairs of passes, each pair of which yields data continuous in time that traces out both noon and midnight latitude profiles within a period of $\sim$ 30 minutes. This is as close as one can come with one satellite to simultaneous observation of the noon and midnight profiles and eliminates a great deal of scatter due to time variations associated with magnetic activity.

It is now possible to fit this observed diurnal variation by adjusting the magnetic field configuration to yield the appropriate drift paths while conserving $\mu$, J and E. This was done by using a dayside configuration (Mead, 1964) which agrees with experimental observations (Ness et al., 1964) and adjusting the nightside configuration to fit the results of the charged particle observations.

The solid line through the data in Figure 5 shows the predicted amount of shift from the model magnetosphere considered to yield the most reasonable results of the configurations tested. The resultant magnetosphere is shown in Figure 6. It is seen to contain a current sheet coincident with the nightside magnetic equator which separates solar directed fields in the northern hemisphere from anti-solar directed fields in the southern hemisphere. The dahsed lines show the field due to the current sheet alone, $B_{CS}$, while the solid lines give the resultant field consisting of $B_{CS}$, the earth's dipole field ($B_d$), and the field due to magnetospheric boundary currents ($B_S$). The midnight meridian high latitude trapping boundary, defined by field line closure, occurs at 67° at an

altitude of 1100 km and agrees with the observed nightside boundaries for both ≥ 40 kev and ≥ 280 kev electrons.

The current sheet shown in Figure 6 extends from 10 $R_e$ (earth radii) to 40 $R_e$ and has a strength of 40 $\gamma$ immediately adjacent to the sheet. These parameters cannot be uniquely determined by this type of analysis. We therefore show in Table II additional current sheet configurations which will fit the observed diurnal variations. Note that these field strengths are somewhat larger, on the average, than those observed from $\sim$ 10 $R_e$ to 30 $R_e$ in the tail (Ness, 1965).

TABLE II

Current Sheet Characteristics

| Inner Edge ($R_E$) | Outer Edge ($R_E$) | Strength (gamma) |
|---|---|---|
| 10 | 40 | 40 |
| 8 | 40 | 33 |
| 8 | 100 | 23 |

This field configuration, its characteristics and shortcomings have been discussed in some detail by Williams and Mead (1965). Improvements include the use of a more appropriate current sheet in the model, the inclusion of a possible ring current, and a readjustment of the coefficients defining the field due to the boundary currents.

However, the similarity of the field shown in Figure 6 to recent observations (Ness, 1965) and recent theoretical suggestions (Dessler and Juday, 1965; Axford et al., 1965) leads us to conclude that during periods of magnetic quiet, energetic ($E_e \geq 280$ kev) trapped electrons in the outer zone behave in a manner consistent with their drift in the distorted geomagnetic field, under conservation of the adiabatic invariants, $\mu$ and $J$, and the energy, $E$.

We next present observations of the storm time behavior of energetic outer zone electrons which demonstrate the close interplay existing between the trapping regions and the extended geomagnetic tail.

## STORM TIME VARIATIONS

Early measurements of the high latitude boundary of trapped, ≥ 40 kev electrons at low altitude showed that this boundary moves to lower latitudes during periods of intense magnetic activity (Maehlum and O'Brien, 1963). This effect seems to occur for 40 kev electrons, on both the dayside and nightside hemispheres. A movement to lower latitudes during high magnetic activity, of the midnight meridian high latitude boundary of trapped, ≥ 280 kev electrons has also been reported (Williams and Palmer, 1965). However, for these higher energy electrons, the noontime high latitude boundary does not seem much disturbed throughout the period of magnetic activity. Sometime after the peak of activity (a few days), the noontime trapping boundary appears to move slightly to higher latitudes, an effect which may be simply a manifestation of an overall increase in trapped particle intensities (Williams and Palmer, 1965).

The initial results of a study now underway have shown that during a magnetic storm the midnight latitude profile of trappped electrons at 1100 km behaves in a manner consistent with the behavior of the magnetic tail field at 30 $R_e$ (Ness and Williams, 1965). These results are obtained by using simultaneous observations of trapped electrons by the APL satellite 1963 38C and of the magnetic field by the NASA satellite IMP-1. We shall review these results and present evidence that this storm time behavior appears to be a predictable pattern.

Figure 7 shows a sequence of midnight meridian passes, again displayed as count rate versus latitude plots, obtained prior to, during, and after a period of magnetic activity occurring on March 30, 1964. A plot of the planetary $K_p$ index is given at the top of the Figure. We see that passes a and b, obtained prior to the disturbance, display latitude profiles similar to those observed during periods of magnetic quiet (Williams and Palmer, 1965; Williams and Mead, 1965). Pass c, obtained during the disturbance, shows a distinct collapse of the outer boundary to lower latitudes. Pass d, obtained after the disturbance, shows that the boundary has moved back toward the pre-storm value.

A sequence of passes analyzed earlier for the magnetic disturbance occurring on April 1, 1964, shows the same characteristic behavior as above (Ness and Williams, 1965). In both cases (the storms of March 30, 1964 and April 1, 1964) no new particles had appeared at the time of the collapse of the outer boundary to lower latitudes. However, after the disturbance (passed in Figure 7), fresh particles appear throughout these trapping regions.

The behavior of the midnight high latitude boundary for trapped $\geq$ 280 kev electrons (defined at 1 count per sec and shown as small dashes in Figure 7) is shown in Figure 8 for the period March 29 through April 2, 1964. A plot of the $K_p$ index is included. The dramatic lowering of the midnight trapping boundary during magnetically active periods is clearly observed. During this period, the satellite was within $4^\circ$ of the midnight meridian.

The collapse of the trapping boundary to lower latitudes during a magnetic disturbance may be caused by formerly closed lines of force being extended into the tail region during the disturbance. Particles trapped on these field lines will be thus injected into the distant magnetic field, possibly forming some of the electron "patches" observed recently in these regions (Anderson et al., 1965).

Analyzing the data for the April 1, 1964 disturbance, Ness and Williams (1965) found that coincident with the surface magnetic activity and the trapped electron boundary collapse, the field strength at 30 $R_e$ in the tail increased. Using a time history of the field magnitude in the tail, it was possible to obtain a midnight trapping boundary for electrons by analyzing field line closure in the field model of Figure 6 (Williams and Mead, 1965). These results are reproduced here in Figure 9.

The tail field magnitude is given by three hour averages and is seen to strongly correlate with $K_p$. The disturbance on April 1, 1964 is clearly seen in the tail field magnitudes and the $K_p$ values. The predicted midnight trapping boundary is shown and was obtained using the following current sheet parameters: inner edge, 8 $R_e$; outer edge, 200 $R_e$ and field strengths as shown in Figure 9. The measured trapping boundaries a, b, c and d, correspond to passes obtained at a, 0651 hrs 31 March 1964; b, 0608 hrs 1 April 1964; c, 0000 hrs 2 April 1964; d, 0526 hrs 2 April 1964.

While the absolute position of the predicted and measured boundaries differ by an average of about five degrees, it is seen that the magnitude of the boundary collapse during the disturbance can be

explained by the behavior of the tail field. The discrepancy in absolute position has been noted and discussed previously (Williams and Mead, 1965; see model improvements listed in previous section).

We have thus seen that, using a tail field model of the magnetosphere and assuming motion of charged particles conserving $\mu$, J and E, the behavior of the midnight latitude profile for energetic electrons as observed at 1100 km is consistent with the behavior of the magnetic field some 30 $R_e$ in the tail. Moreover, the magnitude of the latitude shift is in fair quantitative agreement with the results of a field model using a tail like structure.

The data of Figures 7 and 8 imply that this is a predictable effect and is not a special event unique to the April 1, 1964 disturbance. A general study is now underway using all available simultaneous data from the satellites 1963 38C and IMP-1.

## CONCLUDING REMARKS

Evidence of a 27 day cycle in the intensities of energetic ($E_e \geq$ 280 kev) trapped electrons has been presented. This effect occurs throughout much of the outer zone, $L \geq 3.5$. Occurring near the minimum of solar activity, this effect shows clearly the sensitive interplay between the radiation cavity and the properties of the solar wind and of the interplanetary magnetic field. The correlation of these intensity increases with the passage of the recently observed interplanetary magnetic field sectors (Ness and Wilcox, 1965) was also demonstrated.

It was further shown that the behavior of trapped, energetic electrons during periods of magnetic quiet is consistent with their motion in the distorted geomagnetic field, under conservation of the adiabatic invariants. Using this result, it was then shown that, during magnetic storms, the observed behavior of the midnight meridian high latitude trapping boundary of $\geq$ 280 kev electrons is consistent with the observed behavior of the tail field.

Many problems still exist in connection with these trapped energetic electrons. Where do they come from? Are the observed intensity increases due to injection at low energy from the solar wind into the magnetosphere and subsequent acceleration within the magnetosphere, or are the intensity increases due to local acceleration mechanisms? By observing the spatial and energy dependence of the low altitude trapped electron intensity increases, one "feels" that no single mechanism

is responsible for these changes throughout the entire trapping region (Williams and Smith, 1965). Rather, different mechanisms may dominate in various regions of the magnetosphere. What are some of these "acceleration mechanisms" capable of accelerating electrons to many Mev in energy? What are the loss processes causing the observed lifetimes in the outer zone (Williams and Smith, 1965)? Why isn't the dayside trapping boundary for $\geq$ 280 kev electrons much perturbed during magnetic disturbances? Can electric fields, capable of accelerating electrons some tens of kev but not hundreds of kev (Taylor and Hones, 1965), explain the many differences between the behavior of $\geq$ 40 kev and $\geq$ 280 kev trapped electrons (O'Brien, 1964; Williams and Mead, 1965)?

With improved measurements and the availability of quantitative models for comparison, we hope to see many of the questions answered during the oncoming solar maximum. One of the most important tools in these analyses will be the use of simultaneous observations at various observation points throughout the magnetosphere.

The Johns Hopkins University
APPLIED PHYSICS LABORATORY
Silver Spring, Maryland



## ACKNOWLEDGMENTS

This work was supported in part by the Bureau of Naval Weapons, Department of the Navy, under contract NOw 62-0604-c and in part by a National Aeronautics and Space Administration Grant.

# FIGURE CAPTIONS

Figure 1: Trapped electron intensities for the four consecutive solar rotations beginning October 6, 1963. The data are for L = 4.5 and 1100 km. The occurrence of the interplanetary magnetic field sector boundaries is also shown, + = field away from sun, - = field toward sun (Ness and Wilcox, 1965). The trapped electron intensities are seen to display a clear 27-day variation with increasing intensities occurring as a sector boundary sweeps past the earth. There is also evidence for a second increase occurring $\sim 180°$ (13 1/2 days) after the initial increase in a given rotation period.

Figure 2: Same as Figure 1: L = 4.5 $E_e \geq 1.2$ Mev. Note time lag between appearance of these higher energy electrons and the lower energy electrons in Figure 1.

Figure 3: Same as Figure 1: L = 3.0 $E_e \geq 280$ kev. Note steady decay except for occurrences of sudden intense magnetic activity.

Figure 4: Day and night count rate versus $\Lambda$ plots for the magnetically quiet period October 2-12, 1963. Curves are shown for both $E_e \geq 280$ kev and $\geq 1.2$ Mev. $\Lambda$ is defined at satellite altitude: $\cos \Lambda = \sqrt{\frac{1.17}{L}}$. (From Williams and Mead, 1965)

Figure 5: Plot of latitude shift, $\Delta\Lambda = \Lambda_D - \Lambda_N$, versus noontime latitude, $\Lambda_D$. Bars on data points represent entire spread of data seen

during the period October 2-12, 1963. Solid curve is the predicted latitude shift obtained from the magnetosphere model of Figure 6. (From Williams and Mead, 1965)

Figure 6: Magnetospheric configuration fitting the trapped electron diurnal variation observations. Solid lines show field lines resulting from addition of a current sheet in the tail of the field model originally discussed by Mead (1964). Dashed lines show field lines due to the current sheet alone. (From Williams and Mead, 1965).

Figure 7: Four passes displayed as count rate vs. $\Lambda$ plots obtained near midnight meridian showing collapse of outer boundary during magnetic storm. Pass times indicated on the $K_p$ plot are a: 0633 hrs March 29 (Day 89), 1964; b: 1001 hrs March 29 (Day 89), 1964; c: 1508 hrs March 30 (Day 90), 1964; d: 0651 hrs March 31 (Day 91), 1964.

Figure 8: Behavior of the outer trapping boundary (defined at 1 count per sec) during the period March 29 through April 2, 1964 and its correlation with $K_p$.

Figure 9: Plot showing $K_p$ variation, tail field magnitude and direction at 30 $R_e$ and the predicted and observed outer trapping boundary throughout the disturbance of April 1, 1964. (From Ness and Williams, 1965)

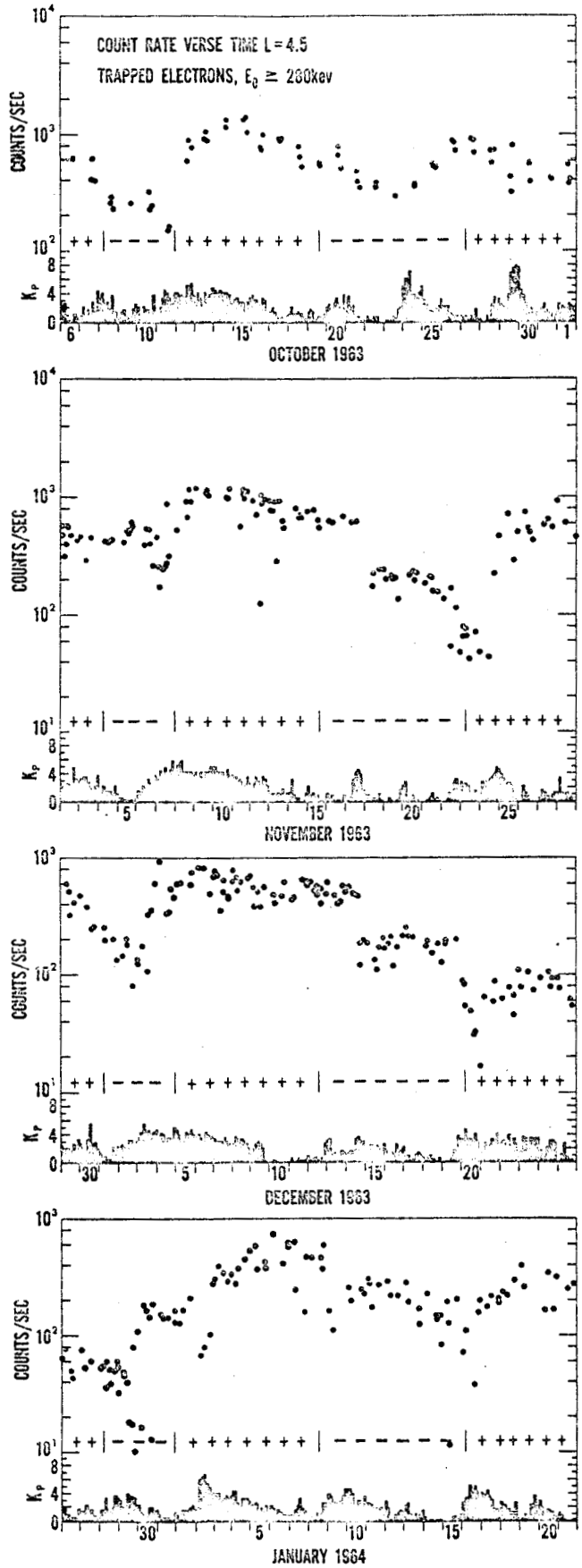
COUNT RATE VERSE TIME L = 4.5
TRAPPED ELECTRONS, $E_e \geq 280$kev
COUNTS/SEC
$K_p$
OCTOBER 1963
NOVEMBER 1963
DECEMBER 1963
JANUARY 1964

Figure 1

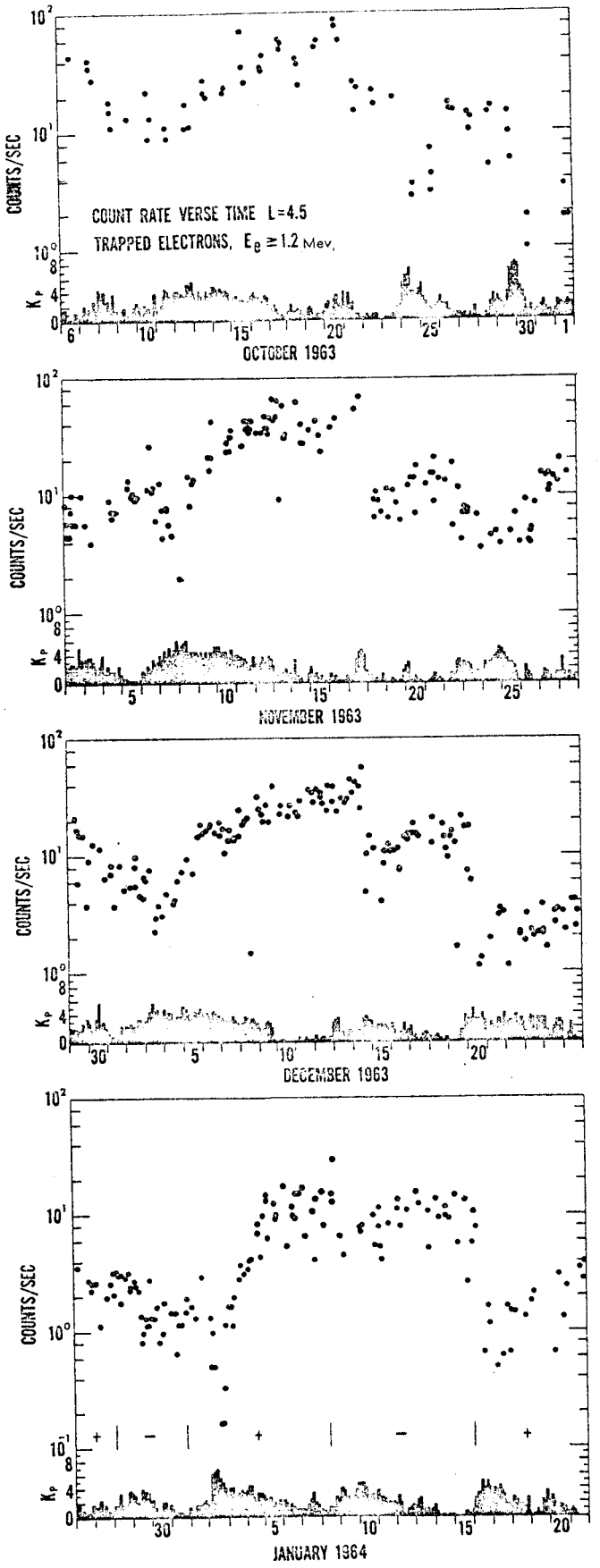
COUNTS/SEC
COUNT RATE VERSE TIME L=4.5
TRAPPED ELECTRONS, $E_e \geq 1.2$ Mev,
$K_p$
OCTOBER 1963
NOVEMBER 1963
DECEMBER 1963
JANUARY 1964

Figure 2

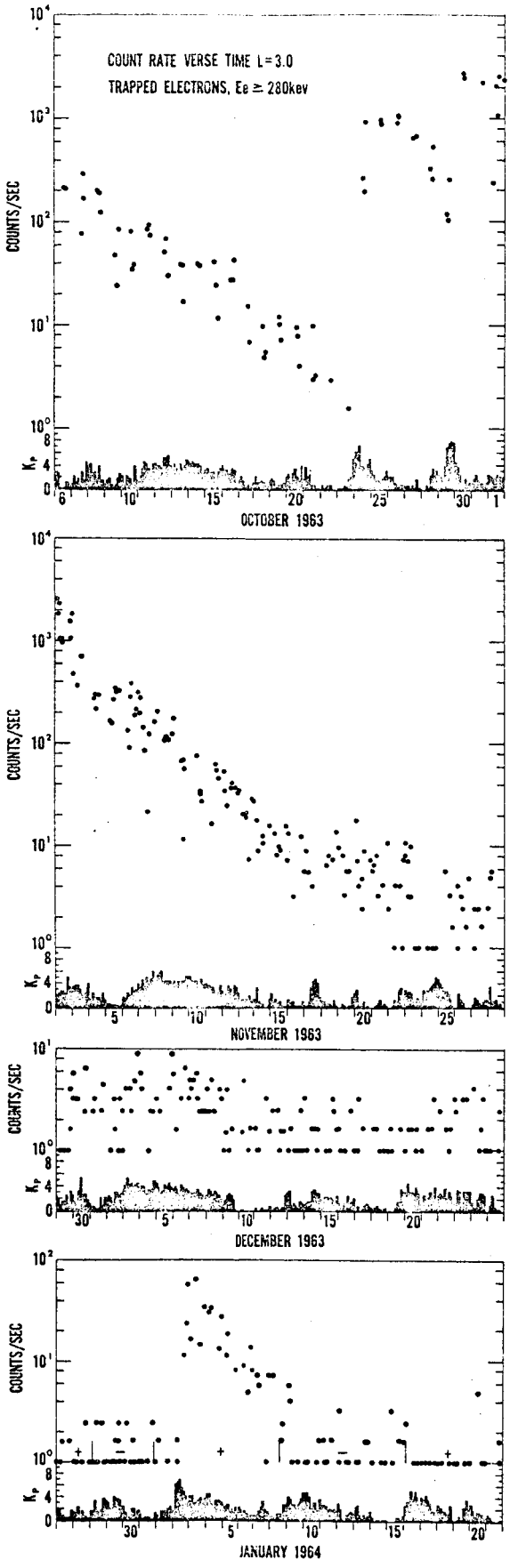
COUNT RATE VERSE TIME L=3.0
TRAPPED ELECTRONS, Ee ≥ 280kev
COUNTS/SEC
$K_p$
OCTOBER 1963
NOVEMBER 1963
DECEMBER 1963
JANUARY 1964

Figure 3

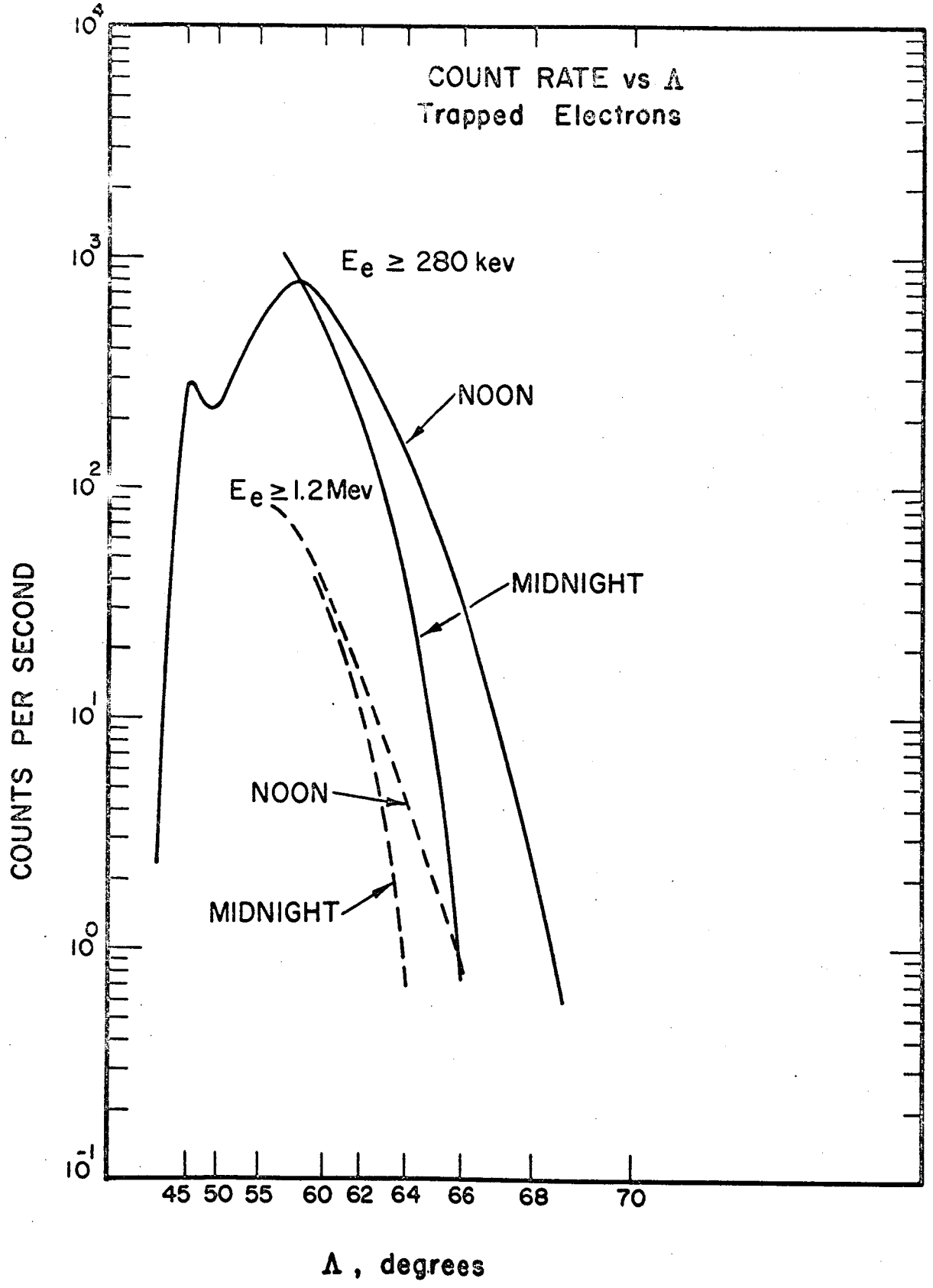
COUNT RATE vs Λ
Trapped Electrons
$E_e \geq 280$ kev
NOON
$E_e \geq 1.2$ Mev
MIDNIGHT
NOON
MIDNIGHT
COUNTS PER SECOND
$10^4$
$10^3$
$10^2$
$10^1$
$10^0$
45 50 55 60 62 64 66 68 70
Λ , degrees

Figure 4

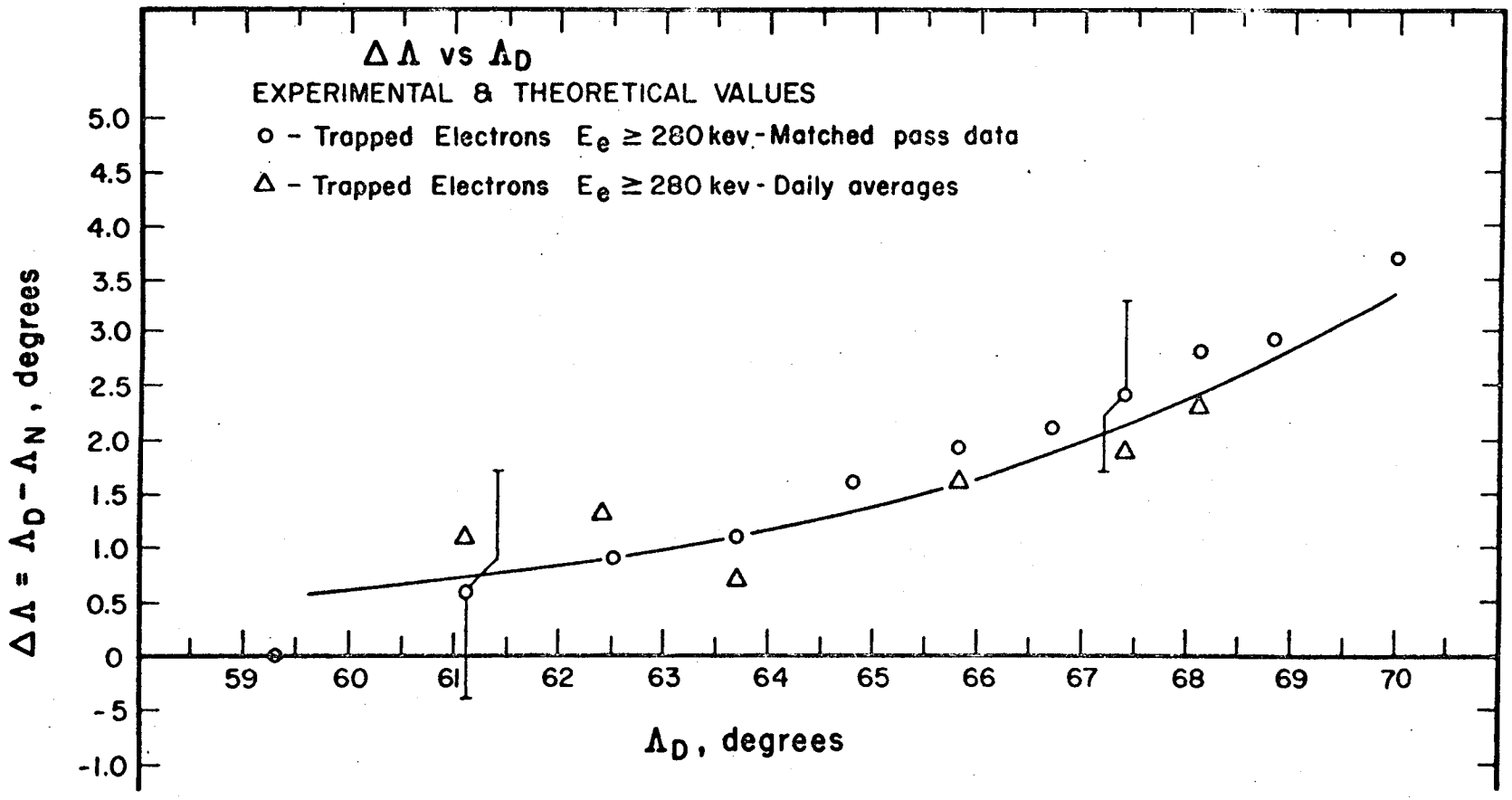
ΔΛ vs Λ_D
EXPERIMENTAL & THEORETICAL VALUES
o - Trapped Electrons E_e ≥ 280 kev - Matched pass data
Δ - Trapped Electrons E_e ≥ 280 kev - Daily averages
ΔΛ = Λ_D - Λ_N , degrees
5.0
4.5
4.0
3.5
3.0
2.5
2.0
1.5
1.0
0.5
0
-5
-1.0
59
60
61
62
63
64
65
66
67
68
69
70
Λ_D , degrees

Figure 5

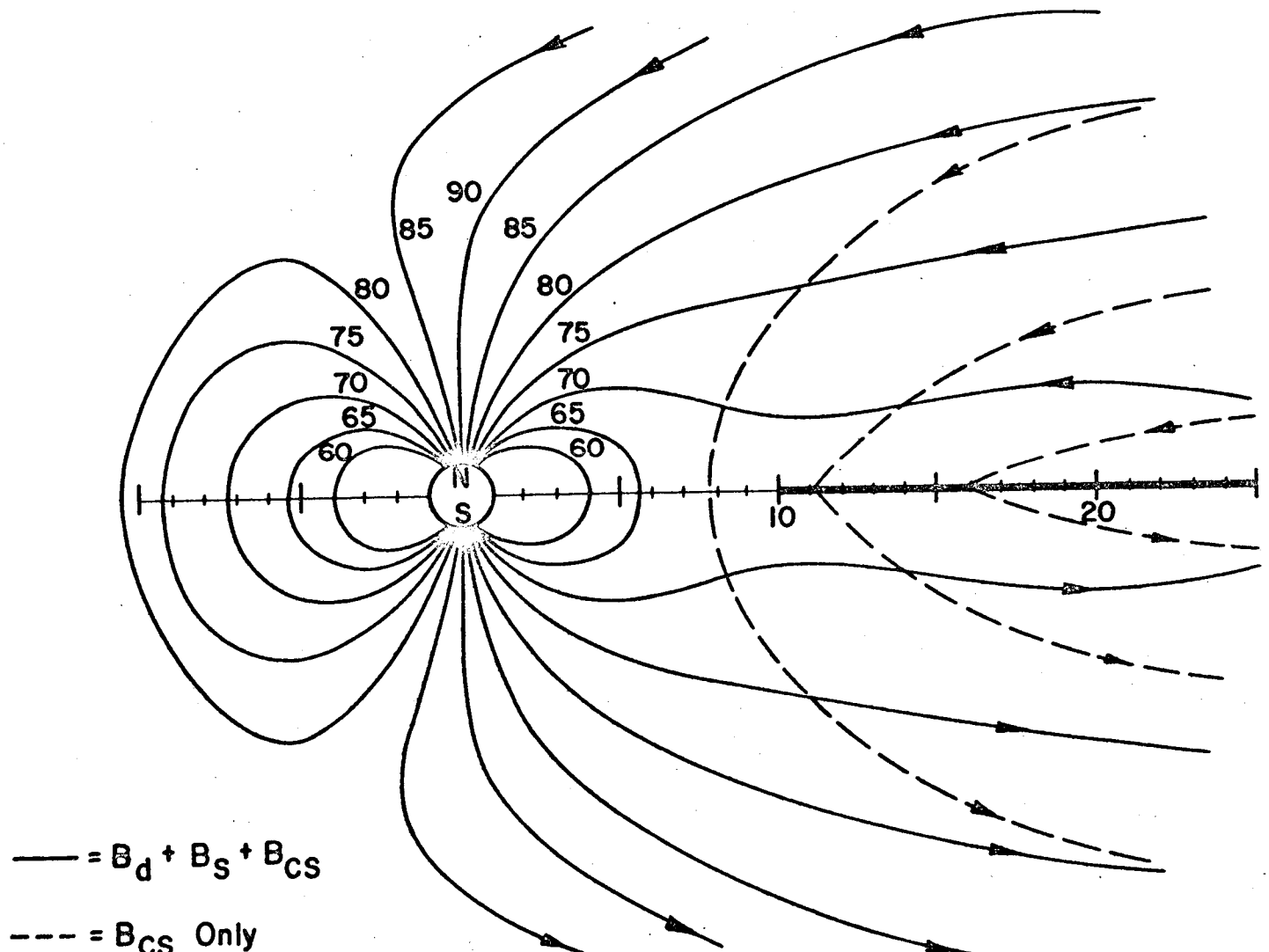


Figure 6

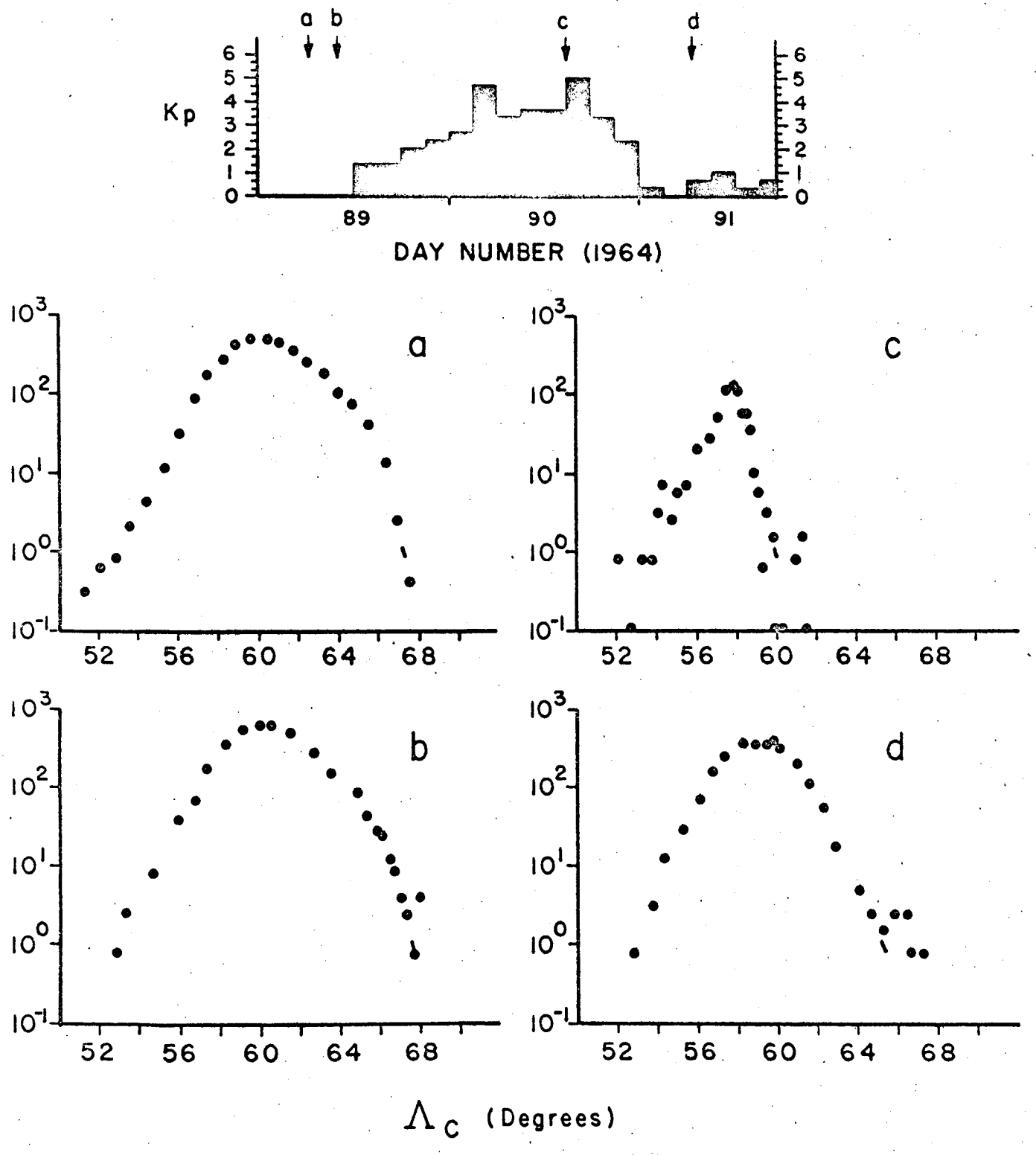
a b
c
d
Kp
6
5
4
3
2
1
0
89
90
91
DAY NUMBER (1964)
$10^3$
$10^2$
$10^1$
$10^0$
$10^{-1}$
a
c
b
d
52
56
60
64
68
$\Lambda_c$ (Degrees)

Figure 7

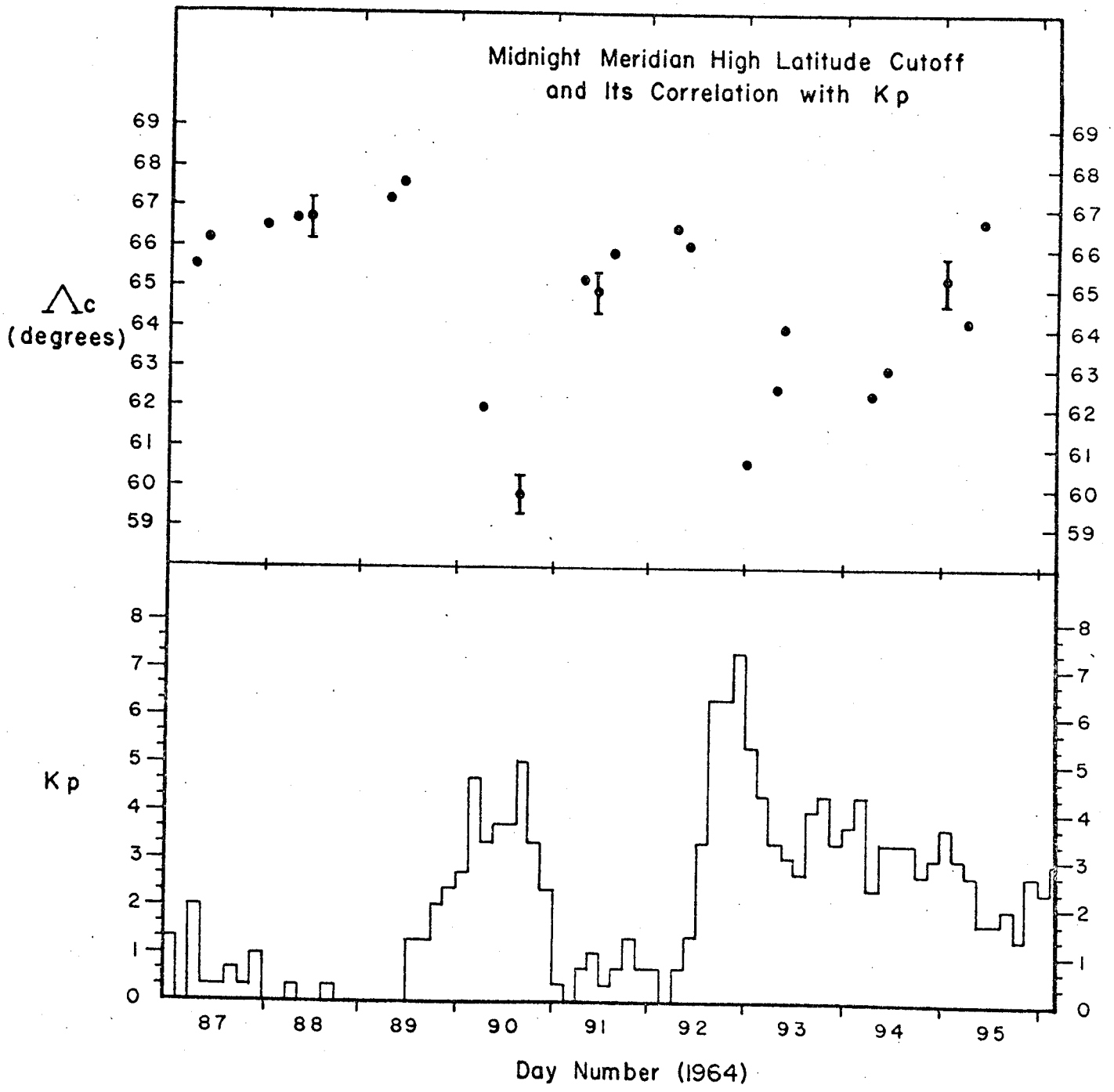
Midnight Meridian High Latitude Cutoff
and Its Correlation with Kp
Λc
(degrees)
69
68
67
66
65
64
63
62
61
60
59
Kp
8
7
6
5
4
3
2
1
0
87
88
89
90
91
92
93
94
95
Day Number (1964)

Figure 8

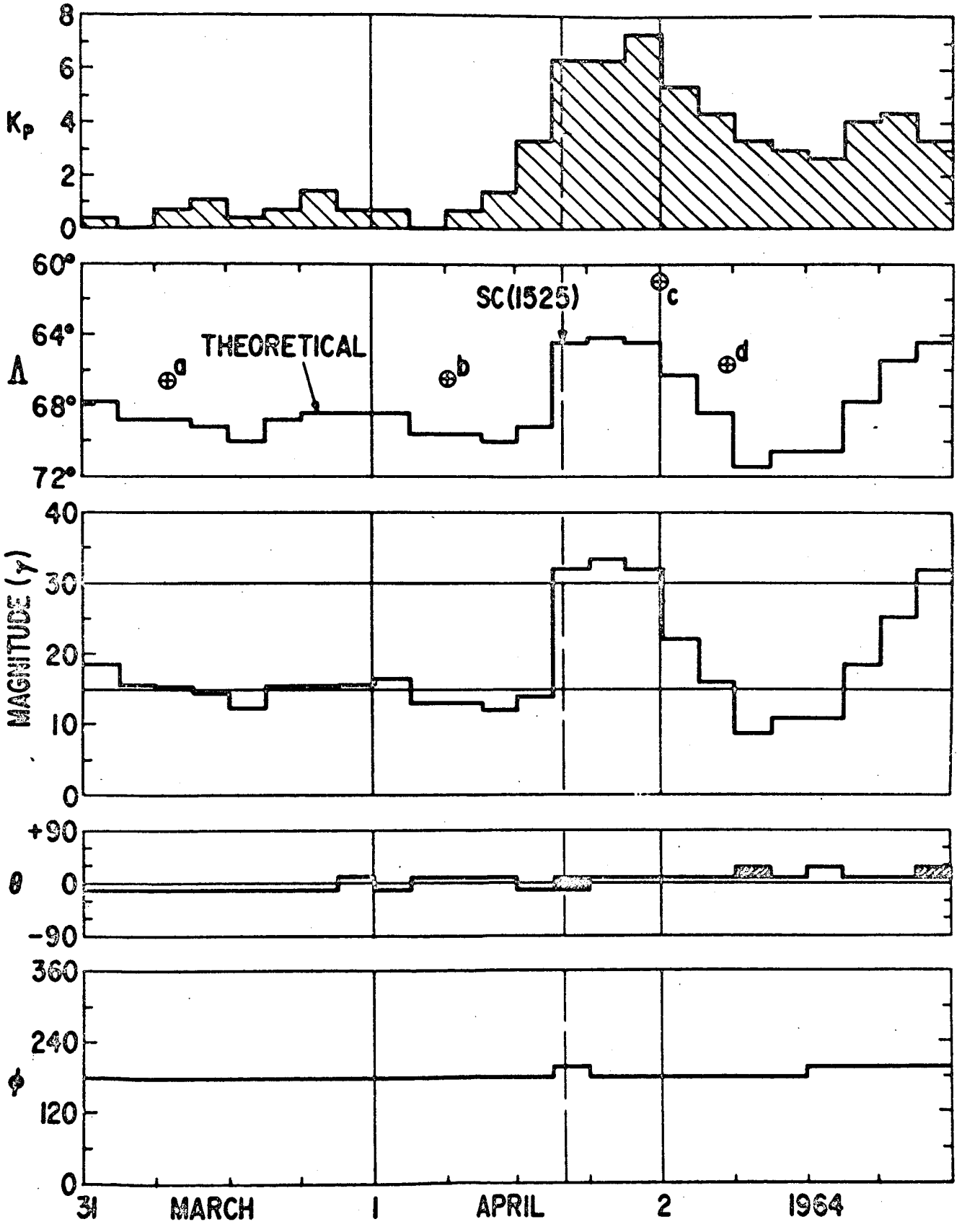
8
6
$K_p$
4
2
0
60°
64°
Λ
68°
72°
SC(1525)
c
THEORETICAL
a
b
d
40
30
MAGNITUDE (γ)
20
10
0
+90
θ
0
-90
360
240
φ
120
0
31
MARCH
1
APRIL
2
1964

Figure 9

The Johns Hopkins University
APPLIED PHYSICS LABORATORY
Silver Spring, Maryland



## REFERENCES

Anderson, K. A., Harris, H. K. and Paoli, R. J.: J. Geophys. Res., 70, 1039 (1965)

Armstrong, T.: J. Geophys. Res., 70, 2077 (1965)

Axford, W. I., Petschek, H. E. and Siscoe, G. L.: J. Geophys. Res., 70, 1231 (1965)

Dessler, A. J. and Juday, R. D.: Planetary Space Sci., 13, 63 (1965)

Frank, L. A., Van Allen, J. A. and Craven, J. D.: J. Geophys. Res., 69, 3155 (1964)

Frank, L. A.: University of Iowa Report 65-14, May 1965

Fritz, T. A. and Gurnett, D. A.: J. Geophys. Res., 70, 2485 (1965)

Maehlum, B. and O'Brien, B. J.: J. Geophys. Res., 68, 997 (1963)

McDiarmid, I. B. and Burrows, J. R.: Can. J. Phys. 42, 616 (1964a)

McDiarmid, I. B. and Burrows, J. R.: Can. J. Phys., 42, 1135 (1964b)

McDiarmid, I. B. and Burrows, J. R.: J. Geophys. Res., 70, 3031 (1965)

Mead, G. D.: J. Geophys. Res., 69, 1181 (1964)

Ness, N. F., Scearce, C. S. and Seek, J. B.: J. Geophys. Res., 69, 3531 (1964)

Ness, N. F. and Wilcox, J. M.: Goddard Space Flight Center Report No. X-612-65-157, April 1965

Ness, N. F.: J. Geophys. Res., 70, 2989 (1965)

Ness, N. F. and Williams, D. J.: to be published Phys. Rev. Letters (1965)

O'Brien, B. J.: J. Geophys. Res., 67, 3687 (1962)

O'Brien, B. J.: J. Geophys. Res., 68, 989 (1963)

O'Brien, B. J.: J. Geophys. Res., 69, 13 (1964)

O'Brien, B. J. and Taylor, H.: J. Geophys. Res., 69, 45 (1964)

Taylor, H. E. and Hones, E. W.: University of Iowa Report 65-10, April 1965

Williams, D. J. and Smith, A. M.: J. Geophys. Res., 70, 541 (1965)

Williams, D. J. and Palmer, W. F.: J. Geophys. Res., 70, 557 (1965)

Williams, D. J. and Mead, G. D.: J. Geophys. Res., 70, 3017 (1965)